

## Concentrating Genomic Length DNA in a Microfabricated Array

Yu Chen,<sup>1,2</sup> Ezra S. Abrams,<sup>4</sup> T. Christian Boles,<sup>4</sup> Jonas N. Pedersen,<sup>5</sup> Henrik Flyvbjerg,<sup>5</sup>  
Robert H. Austin,<sup>1,3,\*</sup> and James C. Sturm<sup>1,2</sup>

<sup>1</sup>Princeton Institute for Science and Technology of Materials (PRISM), Princeton, New Jersey 08540, USA

<sup>2</sup>Department of Electrical Engineering, Princeton University, Princeton, New Jersey 08544, USA

<sup>3</sup>Department of Physics, Princeton University, Princeton, New Jersey 08544, USA

<sup>4</sup>Sage Science, Inc., Beverly, Massachusetts 01915, USA

<sup>5</sup>Department of Micro- and Nanotechnology, Technical University of Denmark, DK-2800 Kongens Lyngby, Denmark

(Received 4 October 2014; revised manuscript received 27 January 2015; published 15 May 2015)

We demonstrate that a microfabricated bump array can concentrate genomic-length DNA molecules efficiently at continuous, high flow velocities, up to 40  $\mu\text{m/s}$ , if the single-molecule DNA globule has a sufficiently large shear modulus. Increase in the shear modulus is accomplished by compacting the DNA molecules to minimal coil size using polyethylene glycol (PEG) derived depletion forces. We map out the sweet spot, where concentration occurs, as a function of PEG concentration and flow speed using a combination of theoretical analysis and experiment. Purification of DNA from enzymatic reactions for next-generation DNA-sequencing libraries will be an important application of this development.

DOI: 10.1103/PhysRevLett.114.198303

PACS numbers: 82.35.Lr, 82.35.Pq, 87.80.Qk, 87.85.gf

The first step in mapping and sequencing a genome, or parts of it, is typically extraction of genomic-length double-stranded DNA molecules from cells. These extremely long molecules have contour lengths of 10–1000  $\mu\text{m}$ , and there are basically two ways to sort and concentrate them according to length: (i) by gel electrophoresis at very low fields (and correspondingly long, multiday run times) to avoid elongation of the spherical random coils that these molecules form in solution [1], (ii) by full elongation either in crossed fields [2,3] or via stretching in nanochannels [4].

While stretching of the DNA, either in post arrays or in nanochannels, is an attractive technology that is rapidly growing in popularity [5], it does not easily scale to high single-molecule throughput, which is needed for preparative work [6]. However, most techniques that do not deliberately stretch the DNA rely on a conformation of the molecule that is as close to spherical as possible. Indeed, the first attempt to sort DNA in a nanofabricated device [7] failed precisely because DNA is so easily elongated in shear fields. Thus, the shear elongation of very long DNA molecules is not only a fascinating problem in polymer physics, its understanding and modulating is also of great impact in biotechnology where failure to control the shear moduli in large biopolymers can be very costly.

Here we raise and control the shear modulus of coils of genomic-length DNA well enough to concentrate them up to 87-fold at high speed and continuous flow. This is the first step towards high-speed, high-throughput sorting of such DNA according to length with the same technology.

**Bump arrays and shear flow.**—A bump array, also known as a deterministic lateral displacement array is a microfluidic device consisting of a central region with posts

placed on a grid with a row shift (Fig. 1). Particles smaller than a critical size  $D_c$  follow the laminar flow direction, weaving through the post array in a “zigzag” trajectory, while particles larger than the critical size are displaced laterally by the posts at each column. Consequently, they will follow the migration angle  $\theta$  in a “bumping” trajectory [8–13]. Previously, it was demonstrated how a bump array can sort solid polystyrene beads according to size

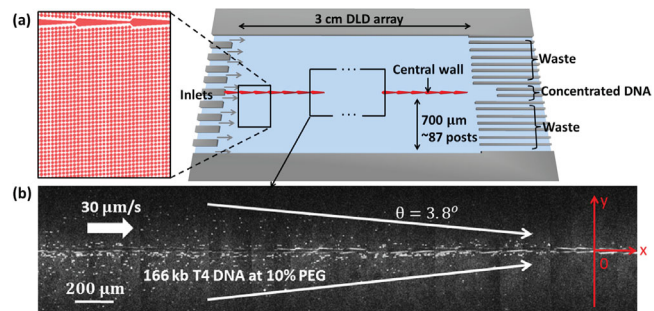


FIG. 1 (color online). DNA concentrator using bump arrays with migration angle  $\theta = 3.8^\circ$ . (a) Schematic of the array. (The real array is 21 times longer than wide: approximately 3 cm long, 1.4 mm wide, 10  $\mu\text{m}$  deep, and symmetric about the central wall.) DNA molecules enter via the inlet region, concentrate along the central (red) wall, and are collected at the product outlets. Red enlargement = array of circular posts arranged in rows that are tilted towards the wall, which is also shown. All particles that follow the  $3.8^\circ$ -tilted rows of posts, have concentrated at this wall when they have flowed 1 cm into the array, for a net concentration of  $\times 87$  before exiting the array. (b) Micrograph composite of purified 166 kbp T4 DNA in a solution with 10% PEG (w/v) in a flow with a peak speed of 30  $\mu\text{m/s}$ . The DNA concentrates along the central wall as it moves through the bump array.

[14]. The same technique is being used with high throughput to separate cancer cells from blood [13,15].

The separation method of the bump array relies on particles being globular, and not easily deformable by the flow. Minimal deformation is important because particles should be pushed (bumped) into adjacent stream lines by posts blocking their flow along stream lines, giving rise to nonhydrodynamic forces which break time and velocity inversion symmetry. Particles too small or too soft will follow the laminar flow in its zigzag trajectory around posts. A coiled polymer “particle” may elongate along the flow lines in response to the shear forces that it encounters in the array. If it is elongated so much that its short axis is shorter than the critical size, it will follow the zigzag path of the flow lines through the array, and hence not displace laterally.

**PEG compacts DNA by depletion force.**—Polyethylene glycol (PEG) is often used for DNA compaction and precipitation [16–20]. PEG’s presence causes an attractive depletion force [21] between surfaces less than one PEG diameter apart and hence between such parts of DNA in a coil that can come close to each other (Fig. 2).

The possibility of using depletion force to hold long DNA molecules in a relatively firm globular conformation should allow use of rapid, scalable continuous-flow methods for DNA manipulation [23,24]. One such application is a DNA concentrator that uses a bump array to concentrate genomic length DNA molecules (Fig. 1).

**Device description.**—Figure 1(a) shows a schematic of the device. It is fabricated in silicon by conventional

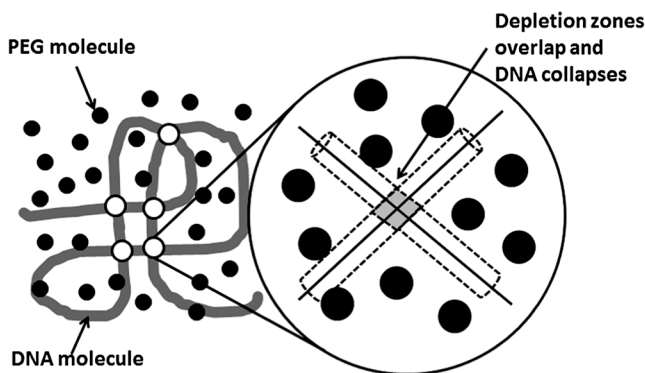


FIG. 2. Depletion force induced by PEG crowding. The centers of PEG molecules cannot come closer to a DNA strand than the radius of a PEG molecule. Thus each DNA molecule is surrounded by a zone that is depleted of centers of PEG molecules: PEG is restricted to the complement of these depletion zones. When depletion zones overlap, they take up less space, and hence their complement is larger. This increase in PEG-accessible volume increases the entropy of the PEG solution, which lowers its free energy. This causes an entropic force that favors increasing overlaps between depletion zones. At low number concentrations  $c$  of PEG, the pressure that compresses overlapping depletion zones is  $ck_B T$  [22]. This compression of depletion zones results in DNA compaction.

photolithography technology and deep anisotropic etching. For details of the array construction and fabrication see [25]. A low-concentration DNA solution enters through the ten inlet channels, flows through the central bump array region where it is concentrated from 87 channels on each side to 1 on each side, and leaves through the 17 outlet channels. The three output channels closest to the wall are the product outlets.

**Experimental results.**—For details of the DNA staining procedure, see Ref. [25]. Figure 3 shows fluorescent micrographs of purified 166 kbp T4 DNA under different conditions in the bump array. At zero fluid speed and with no PEG in the solution, DNA is in a globular conformation as expected, only slightly deformed by the presence of the posts [Fig. 3(a)]. The blue concentric circles have radii of 1 and 2  $\mu\text{m}$ , respectively.

Now consider a fixed fluid flow of, say, 20  $\mu\text{m/s}$  peak speed between posts. The flow shears in the bump array because of the flow’s no-slip boundary condition at the

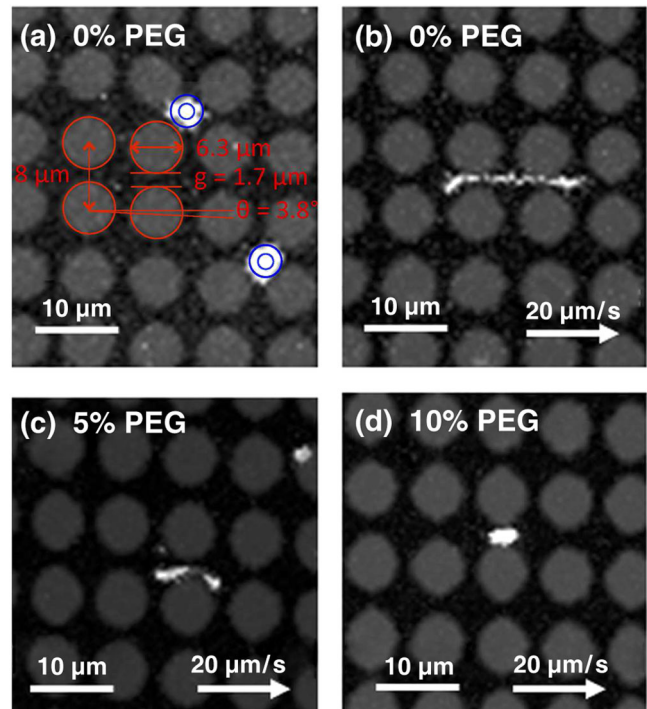


FIG. 3 (color online). Purified 166 kbp T4 DNA in microfluidic array. (a) No PEG added and no flow. The DNA coils up to a spherlike object, slightly deformed by the posts. The concentric circles have radii of  $R_g = 1 \mu\text{m}$  and  $2R_g$ , respectively, with  $R_g$  the estimated radius of gyration. (b),(c),(d) 0%, 5%, and 10% PEG concentrations, respectively, all at flow speed 20  $\mu\text{m/s}$ . In (b) the DNA is elongated by the shear flow and reaches a length of  $\sim 17 \mu\text{m}$ , i.e.,  $\sim 30\%$  of its contour length. It follows the flow through the array. With PEG present, (c),(d), DNA is stretched less by the shear flow. At high PEG concentrations, DNA can maintain a globular conformation in the shear flow; hence, it behaves like a solid particle and is laterally displaced deterministically.

surfaces of the posts. Without PEG in the solution, videos of DNA's motion through the array show that the DNA changes dynamically between globular and elongated conformations, see video in Ref. [25], as previously observed in shear flows [26]. We use the easily measured extent of the molecule in the direction of the flow to characterize its conformation (Fig. 4), while its transverse extent, which triggers the bumping or zigzag mode, is difficult to measure.

Figure 3(b) shows an example of a molecule sheared at a peak flow speed of  $v_{x,\max} = 20 \mu\text{m/s}$  and elongated up to  $17 \mu\text{m}$ , i.e.,  $\sim 30\%$  of its contour length. See Ref. [25] for a movie of the motion of a T4-DNA molecule at 0% PEG. The effective width of the sheared molecule is smaller than the critical size of the array, and, consequently, the DNA molecule follows a zigzag path through the array. No lateral displacement takes place (gray area in Fig. 5).

Adding PEG to the solution qualitatively changes the behavior of the DNA in the array. For a flow rate of  $20 \mu\text{m/s}$ , even 5% PEG makes the conformation of DNA less extended, with length  $\sim 8 \mu\text{m}$  [Fig. 3(c)]. This conformation “bumps” through the array, moving along a tilted row of posts (white area in Fig. 5), in contrast to the motion without added PEG [Fig. 3(b)]. However, increasing the PEG concentration to 15% diminishes the size of the DNA to a value below the critical size of the array, and the DNA follows the flow again. Thus, to concentrate DNA at the central wall, the PEG concentration must be tuned so the DNA can resist the shear force in the gaps between the posts, but remains sufficiently large to bump at the posts—the PEG concentration must be within the white area in Fig. 5.

*Theory.*—A coarse statistical model of a DNA molecule in solution is provided by a freely jointed chain of  $N = L/\kappa$  segments, where  $L$  is the contour length of the DNA,

$\kappa = 2L_p$  its Kuhn length, and  $L_p$  its persistence length [27] [Sec. 9c]. For T4 DNA molecules stained with YOYO-1,  $L \approx 1.12 \times 56 \mu\text{m} \approx 63 \mu\text{m}$  [28] and  $L_p = 0.050 \mu\text{m}$ , which gives  $N \approx 630$  segments.

Without PEG in the solution and no flow, this simple model for the DNA conformation predicts that DNA forms a coil that is described as a three-dimensional random walk with  $N$  steps, each step equal to a Kuhn length. This leads to a Gaussian density distribution. The radius of gyration for the coil is  $R_g = \sqrt{R_0^2/6} = \sqrt{\langle \mathbf{R}^2 \rangle / 6} = 2L_p \sqrt{N/6} \approx 1 \mu\text{m}$  [27], where  $\mathbf{R}$  is the end-to-end distance of the molecule. Although this estimate is a lower bound for the size of the molecule since excluded volume effects are not included [30], the diameter of the molecule is larger than the gap between the posts, and it is much larger than the critical diameter  $D_c \approx 0.7 \mu\text{m}$  for hard spheres [25]. Figure 3(a) shows how the posts deform the DNA coil even in the absence of flow.

In the presence of a fluid flow, DNA molecules experience a shear stress from the flow's shear [9]. This shear deforms the DNA as observed in Fig. 3(b). According to theory [32], DNA will elongate when the Weissenberg number  $Wi = \dot{\gamma}\tau \approx 1$ , where  $\dot{\gamma}$  is the applied shear rate, and  $\tau$  is the natural relaxation time of the polymer. Assuming a parabolic flow profile in gaps of width  $g$  between posts [10],  $v_x(y) = v_{x,\max}[1 - (1 - 2y/g)^2]$  for  $0 < y < g$ , and the shear rate in the gap is  $\dot{\gamma} = dv_x/dy = (4v_{x,\max}/g)(1 - 2y/g)$ . That is, the shear rate varies linearly with position between the peak value  $\pm 4v_{x,\max}/g$  at the post walls, and vanishes at the center of the gap.

To estimate the relaxation time, we use the scaling relation [32]

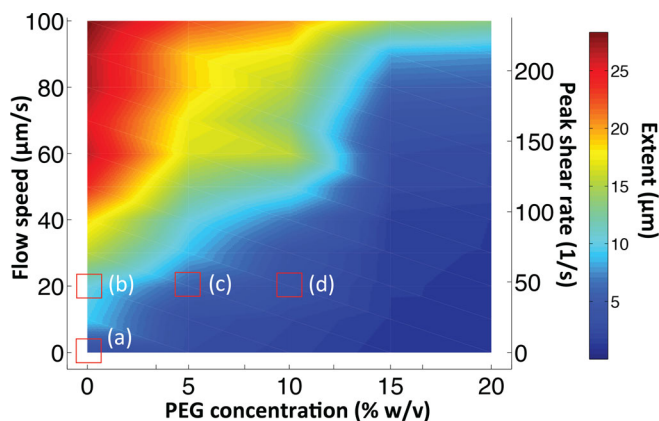


FIG. 4 (color online). Heat map of the average extent along the flow for 166 kbp T4 DNA as a function of PEG concentration and peak flow speed or peak shear rate. This heat map is based on experimental data recorded at 30 points in the plane, those marked with circles in Fig. 5. Letters (a)–(d) refer to panels in Fig. 3.

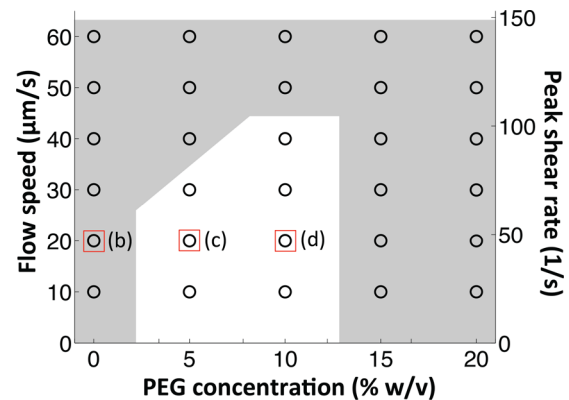


FIG. 5 (color online). Map showing which PEG concentrations and flow speeds or peak shear rates will concentrate 166 kbp T4 DNA (white area) or not (gray area) in the bump array in Fig. 3. The map is based on measurements done at the values marked with open circles. The transition between concentrated output or not is abrupt as a function of the PEG concentration and flow speed because of the large number of posts encountered by a molecule passing through the array [25]. Letters (b)–(d) refer to panels in Fig. 3.



$$\tau \approx \frac{0.2\eta R_{\text{coil}}^3}{k_B T}, \quad (1)$$

where  $\eta = 8.9 \times 10^{-4}$  Pa·s is the viscosity of water, and  $R_{\text{coil}}$  is the unperturbed coil radius. Setting  $R_{\text{coil}}$  equal to the average end-to-end distance  $R_0$  gives the relaxation time  $\tau \approx 0.7$  s. This relaxation time depends crucially on the value of  $R_{\text{coil}}$ , so we compare it with experimental relaxation times for  $\lambda$ -DNA molecules at viscosities  $\eta_\lambda$  60 and 220 times larger than water's [26]. Assuming the scaling relation in Eq. (1) holds and that the size  $R_{\text{coil}}$  of the molecule scales as the square-root of the contour length, we can estimate a relaxation time for a T4-DNA molecule in water from the relation

$$\tau_{\text{T4}} = \frac{\eta_{\text{water}}}{\eta_\lambda} \left( \frac{\sqrt{L_{\text{T4}}}}{\sqrt{L_\lambda}} \right)^3 \tau_\lambda, \quad (2)$$

where  $L_\lambda = 22 \mu\text{m}$  is the contour length of a  $\lambda$ -DNA molecule stained with one YOYO-1 molecule per 4 bp [29]. The measured relaxation times are  $\tau_\lambda = 6.3$  and 19 s at the two viscosities. That gives  $\tau_{\text{T4}} = 0.5$  and 0.4 s, respectively, in good agreement with our estimate.

For  $\tau = 0.7$  s, the corresponding Weissenberg numbers are in the range  $\pm(1.6 \text{ s}/\mu\text{m})v_{x,\text{max}}$ . Even for the lowest experimentally controllable flow velocities,  $v_{x,\text{max}} \sim 10 \mu\text{m/s}$ , is  $\text{Wi} \gg 1$  except in a small region around the center of a gap. So the DNA will undergo a coil-stretch transition when passing through a gap, and no lateral displacement will occur [see Figs. 3(b), 4, and 5].

Now consider the effect of adding a small flexible polymer, such as PEG, to a solution containing DNA. Then the depletion force explained in Fig. 2 sets in. As the concentration of PEG is increased, the DNA undergoes a coil-globule transition [19]. This changes the radius of the DNA molecule from the coil value  $R_g$  at zero PEG to a much smaller value  $R_m$ . The transition has been described both theoretically [21,33] and experimentally; see, e.g., Ref. [17]. The latter showed that the coil-globule transitions happens at a PEG concentration in the range from 11% to 19% with a possible first-order transition, i.e., with a coexisting phase [34].

A simple estimate for the minimum radius  $R_m$  that can be reached by depletion forces is

$$\frac{4\pi}{3} R_m^3 = N v_c, \quad (3)$$

where  $v_c \approx \kappa^2 w$  is the excluded volume of a Kuhn segment [31], and  $w = 10$  nm is the effective width of DNA. Here it is, plausibly, assumed that the persistence length  $L_p$  and effective diameter  $w$  of the DNA are not changed by the compacting caused by the depletion forces. For T4-DNA molecules, the expected value is  $R_m \approx 0.25 \mu\text{m}$ . This is approximately a factor of four smaller than the aqueous

value, and about 3 times larger than the radius both of T4 DNA compacted with PEG-A and visualized with transmission electron microscope [35], and of the T4 capsid head [36]. Importantly, this estimate is also significantly lower than the critical diameter  $D_c \approx 0.7 \mu\text{m}$  for bumping in the array [37].

*Discussion.*—From the heat map in Fig. 4, we can understand the DNA molecules' behavior in bump arrays. For PEG concentrations higher than 10%–15%, DNA molecules have the globular conformation and hence will not be concentrated at the central wall in the bump array used here. They are too small. So instead, they zigzag through the array, following flow lines. For lower PEG concentrations the situation is more complex. Without PEG, the DNA is sheared by even the smallest accessible flow values and becomes elongated, to lengths of 10 micron or more as seen in Fig. 4. In a window of moderate PEG concentrations (5%–10%) and moderate flow velocities ( $v_{x,\text{max}} \lesssim 40 \mu\text{m/s}$ ), the DNA molecules are displaced laterally and concentrate at the central wall (Fig. 5). At these PEG concentrations, the critical peak shear rate  $4v_{x,\text{max}}/g$  is  $\sim 100 \text{ s}^{-1}$ .

The parameter regime for which concentration occurs depends on the geometry of the array. Consider, e.g., decreasing the gap size  $g$  while not reducing  $v_{x,\text{max}}$  proportionally. That will increase the peak shear rate ( $\pm 4v_{x,\text{max}}/g$ ) in the gap, which will (i) lower the maximum flow speed ensuring separation and (ii) increase the PEG concentration needed to prevent the DNA from shearing. Decreasing the gap size  $g$  will also decrease the critical size  $D_c$  of the array [9], which leads to bumping at higher PEG concentrations. In summary, the white area in Fig. 5 is shifted towards higher PEG concentrations and lower flow speeds.

*Summary and outlook.*—We have demonstrated how the extent and shear modulus of DNA conformations can be controlled by depletion force. This control was put to practical use in a bump array that consequently could concentrate DNA molecules in a continuous flow: The DNA was concentrated to a single bump channel, i.e., 87-fold concentration before exiting—with throughput up to  $0.25 \mu\text{L/h}$  (at  $40 \mu\text{m/s}$  in white area in Fig. 5). One can increase the concentration by more than a factor 87 by using a wider array, which also will increase the throughput.

As a potential application, purification of DNA from enzymatic reactions used to produce next-generation DNA sequencing libraries typically require a series of enzymatic processing steps, each step ending with purification of the DNA products away from the modifying enzyme. Since the processing enzymes are orders of magnitude smaller than their DNA substrates, bump arrays provide a promising mechanism for DNA purifications in a flow-based microfluidic system. At the right combination of flow rate and PEG concentration, processed DNA products will bump laterally through the bump array, preferably into collection

channels containing enzyme-free buffer, while the enzymes follow the laminar flow path straight down the array, away from the DNA [40].

This work was supported by the National Institutes of Health Grant No. 1R43HG006818-01 to Sage Science, and National Cancer Institute Grant No. U54CA143803 to Princeton University. The content is solely the responsibility of the authors and does not necessarily represent the official views of the National Cancer Institute or the National Institutes of Health. The work at DTU was supported by the European Union's Seventh Framework Programme No. FP7/2007-2013 under Grant No. 278204 (Cell-O-Matic), and the Danish Council for Strategic Research Grant No. 10-092322 (PolyNano).

\*Corresponding author.

austin@princeton.edu

- [1] T. A. J. Duke, *J. Chem. Phys.* **93**, 9049 (1990).
- [2] O. Bakajin, T. A. J. Duke, J. Tegenfeldt, C.-F. Chou, S. S. Chan, R. H. Austin, and E. C. Cox, *Anal. Chem.* **73**, 6053 (2001).
- [3] L. R. Huang, J. O. Tegenfeldt, J. J. Kraeft, J. C. Sturm, R. H. Austin, and E. C. Cox, *Nat. Biotechnol.* **20**, 1048 (2002).
- [4] J. O. Tegenfeldt, C. Prinz, H. Cao, S. Chou, W. W. Reisner, R. Riehn, Y. M. Wang, E. C. Cox, J. C. Sturm, P. Silberzan *et al.*, *Proc. Natl. Acad. Sci. U.S.A.* **101**, 10979 (2004).
- [5] E. T. Lam, A. Hastie, C. Lin, D. Ehrlich, S. K. Das, M. D. Austin, P. Deshpande, H. Cao, N. Nagarajan, M. Xiao *et al.*, *Nat. Biotechnol.* **30**, 771 (2012).
- [6] E. Borgström, S. Lundin, and J. Lundeberg, *PLoS One* **6**, e19119 (2011).
- [7] W. D. Volkmuth and R. H. Austin, *Nature (London)* **358**, 600 (1992).
- [8] J. A. Davis, D. W. Inglis, K. J. Morton, D. A. Lawrence, L. R. Huang, S. Y. Chou, J. C. Sturm, and R. H. Austin, *Proc. Natl. Acad. Sci. U.S.A.* **103**, 14779 (2006).
- [9] D. W. Inglis, J. A. Davis, R. H. Austin, and J. C. Sturm, *Lab Chip* **6**, 655 (2006).
- [10] D. W. Inglis, J. A. Davis, T. J. Zieziulewicz, D. A. Lawrence, R. H. Austin, and J. C. Sturm, *J. Immunol. Methods* **329**, 151 (2008).
- [11] K. Loutharback, J. Puchalla, R. H. Austin, and J. C. Sturm, *Phys. Rev. Lett.* **102**, 045301 (2009).
- [12] K. Loutharback, K. S. Chou, J. Newman, J. Puchalla, R. H. Austin, and J. C. Sturm, *Microfluid. Nanofluid.* **9**, 1143 (2010).
- [13] K. Loutharback, J. D'Silva, L. Liu, A. Wu, R. H. Austin, and J. C. Sturm, *AIP Adv.* **2**, 042107 (2012).
- [14] L. R. Huang, E. C. Cox, R. H. Austin, and J. C. Sturm, *Science* **304**, 987 (2004).
- [15] N. M. Karabacak *et al.*, *Nat. Protoc.* **9**, 694 (2014).
- [16] T. Biben, P. Bladon, and D. Frenkel, *J. Phys. Condens. Matter* **8**, 10799 (1996).
- [17] J. Pelletier, K. Halvorsen, B.-Y. Ha, R. Paparcone, S. J. Sandler, C. L. Woldringh, W. P. Wong, and S. Jun, *Proc. Natl. Acad. Sci. U.S.A.* **109**, E2649 (2012).
- [18] S. Cunha, C. L. Woldringh, and T. Odijk, *J. Struct. Biol.* **136**, 53 (2001).
- [19] L. S. Lerman, *Proc. Natl. Acad. Sci. U.S.A.* **68**, 1886 (1971).
- [20] S. B. Zimmerman and A. P. Minton, *Annu. Rev. Biophys. Biomol. Struct.* **22**, 27 (1993).
- [21] S. Asakura and F. Oosawa, *J. Polym. Sci.* **33**, 183 (1958).
- [22] P.-G. de Gennes, *Scaling Concepts in Polymer Physics* (Cornell University Press, Ithaca, 1979).
- [23] N. Pamme, *Lab Chip* **7**, 1644 (2007).
- [24] M. D. Tarn, M. J. Lopez-Martinez, and N. Pamme, *Anal. Bioanal. Chem.* **406**, 139 (2014).
- [25] See Supplemental Material at <http://link.aps.org/supplemental/10.1103/PhysRevLett.114.198303> for details on the sample preparation, the parameters of the device, the statistics of bumping, and a description of the movies recorded.
- [26] D. E. Smith, H. P. Babcock, and S. Chu, *Science* **283**, 1724 (1999).
- [27] H. Yamakawa, *Modern Theory of Polymer Solutions*, Harper's Chemistry Series (Harper and Row, New York, 1971).
- [28] Staining with one YOYO-1 molecule per 10 base pairs gives a 12% extension of the contour length [29].
- [29] K. Günther, M. Mertig, and R. Seidel, *Nucleic Acids Res.* **38**, 6526 (2010).
- [30] The thermal blob size of DNA, within which self-avoidance is not felt, is [31]  $\xi_T \approx \kappa^4/v_c \sim 1 \mu\text{m}$ , where  $v_c$  is the excluded volume of a Kuhn segment [see below Eq. (3)]. As  $\xi_T$  is comparable to the radius of gyration  $R_g$ , the freely jointed chain model gives a reasonable approximation for the size of the molecule.
- [31] M. Rubinstein and R. H. Colby, *Polymer Physics* (Oxford University Press, New York, 2003).
- [32] P. G. de Gennes, *J. Chem. Phys.* **60**, 5030 (1974).
- [33] H. Kang, P. A. Pincus, C. Hyeon, and D. Thirumalai, *Phys. Rev. Lett.* **114**, 068303 (2015).
- [34] In Ref. [17] they use PEG-20000, not PEG-8000 as in the present study.
- [35] K. Yoshikawa, Y. Yoshikawa, Y. Koyama, and T. Kanbe, *J. Am. Chem. Soc.* **119**, 6473 (1997).
- [36] N. H. Olson, M. Gingery, F. A. Eiserling, and T. S. Baker, *Virology* **279**, 385 (2001).
- [37] In bulk the dominant state of DNA in the presence of condensing agents is rodlike or globular, but it can enter a toroidal state if the addition of condensing agents is carefully tuned. The toroidal state is also observed in single-molecule experiments with optical tweezers. For details, see Ref. [38] and references therein. A recent study with optical tweezers shows that PEG might also induce a toroidal state [39].
- [38] B. van den Broek, M. C. Noom, J. van Mameren, C. Battle, F. C. MacKintosh, and G. J. L. Wuite, *Biophys. J.* **98**, 1902 (2010).
- [39] H. Ojala, G. Ziedaite, A. E. Wallin, D. H. Bamford, and E. Hægström, *Eur. Biophys. J.* **43**, 71 (2014).
- [40] K. J. Morton, K. Loutharback, D. W. Inglis, O. K. Tsui, J. C. Sturm, S. Y. Chou, and R. H. Austin, *Lab Chip* **8**, 1448 (2008).